

Distributed Learning for MIMO Relay Networks

Rui Wang, *Graduate Student Member, IEEE*, Yi Jiang , *Member, IEEE*, and Wei Zhang , *Fellow, IEEE*

Abstract—This paper studies a multi-antenna multi-user and multi-relay network, where the radio frequency (RF) power amplifiers (PA) of the nodes are subject to instantaneous power constraints. To optimize the nonlinear transceivers of the distributed nodes, we introduce a novel perspective of relating a relay network to an artificial neural network (ANN). With this perspective, we propose a distributed learning-based relay beamforming (DLRB) scheme. Based on a set of pilot sequences, the DLRB scheme can optimize the transceivers to minimize the mean squared error (MSE) of the data stream in a distributed manner. It can effectively coordinate the distributed relay nodes to form a virtual array to suppress interferences, even assuming neither the channel state information (CSI) nor information exchange between the relay nodes or between the users. We also present a frame design to support the DLRB so that it can adapt well with time-varying channels. Extensive simulations verify the effectiveness of the proposed scheme.

Index Terms—Artificial neural network, distributed learning, interference suppression, instantaneous power constraints, relay network.

I. INTRODUCTION

AS A concatenation of a broadcast channel and a multiple access channel, the relay network can help extend communication range and improve channel capacity [1]–[4]. Relay communications have found applications in a wide range of scenarios. For example, in cellular communications, the users at the cell edge with weak signal reception can be compensated by deploying relay nodes to enhance the signal and improve the quality-of-service [5]; in a natural disaster where the regular communication infrastructures are damaged, relay links can be established for emergency communications by deploying relay stations or unmanned aerial vehicles (UAVs) [6], [7]; in

Manuscript received July 31, 2021; revised November 16, 2021; accepted December 30, 2021. Date of publication January 6, 2022; date of current version May 17, 2022. This work was supported in part by the National Natural Science Foundation of China under Grant 61771005, in part by the National Key R&D Program of China under Grant 2020YFA0711400, in part by the Shenzhen Science & Innovation Fund under Grant JCYJ20180507182451820, and in part by the Australian Research Council Project funding scheme under Grant LP160101244. Part of this work was presented at the 2020 Information Theory and Applications Workshop (ITA), and 2020 54th Asilomar Conference on Signals, Systems, and Computers. The guest editor coordinating the review of this manuscript and approving it for publication was Prof. Jun Li. (*Corresponding author: Yi Jiang.*)

Rui Wang and Yi Jiang are with the Key Laboratory for Information Science of Electromagnetic Waves (MoE), Department of Communication Science and Engineering, School of Information Science and Technologies, Fudan University, Shanghai 200433, China (e-mail: ruiwang18@fudan.edu.cn; yijiang@fudan.edu.cn).

Wei Zhang is with the School of Electrical Engineering and Telecommunications, University of New South Wales, Sydney, NSW 2052, Australia (e-mail: w.zhang@unsw.edu.au).

Digital Object Identifier 10.1109/JSTSP.2022.3140953

tactical communications, relay communication is also essential for forming a bunch of distributed nodes into a mesh network [8], [9]. It is also shown that deploying relays between the source, the target terminal, and the eavesdropper can help improve the secrecy rate [10].

In the aforementioned scenarios, the relay nodes are often subject to interferences, inside or outside the network, friendly or hostile, which makes it difficult to obtain the channel state information (CSI), not to mention sharing the information between the relay nodes. Thus, the problem of optimizing a relay network in the presence of interference without using CSI or information sharing between the relay nodes, to the best of our knowledge, remains elusive despite decades of researches on relay networks. This paper focuses on solving this problem.

A. Related Work

Most existing works on the relay network assume that the CSI is known perfectly [11]–[14] or imperfectly [14], [15]. For example, assuming perfect CSI at the receiver sides of the links (CSIR), the authors of [12] derived the optimal beamforming vectors of the source, the relay and the destination to maximize the received signal-to-noise ratio (SNR). Assuming the perfect CSI, the authors of [13] optimized the weight coefficients of the transmitter and the relays to maximize the received SNR. In [16], [17], the authors assumed the second-order statistics of the channel coefficients instead of the perfect CSI. In [15], assuming that the CSI at the sender is imperfect and the norm of the CSI error vector is bounded by a spherical region, the authors proposed a robust optimal collaborative-relay beamforming (CRBF) algorithm by S-Procedure and rank relaxation techniques to maximize the worst-case SNR at the destination.

Interference suppression is growingly important both in cellular communications and emergency/tactical communications, especially as the frequency spectrum becomes increasingly crowded. Fig. 1 just presents two illustrative examples: in Fig. 1(a), the relay nodes can assist the communication between the base station (BS) and a user at the cell edge; in Fig. 1(b), the (UAV) relays can cooperate to establish the communication between a reconnaissance UAV and the command center. In both scenarios, the relays can be subject to the interferences, friendly or hostile. Despite various interesting and critical applications, the literature on interference-resilient relay communications is rather scarce [5], [18]. The authors in [5] considered a cellular communication scenario, where the cell-edge users suffering inter-cell interference can be aided by placing a relay node nearby. They proposed a coordinate ascent algorithm to optimize the covariance matrices of the Gaussian input and the Gaussian quantization noise. But it assumed perfectly-known CSI. In [18],

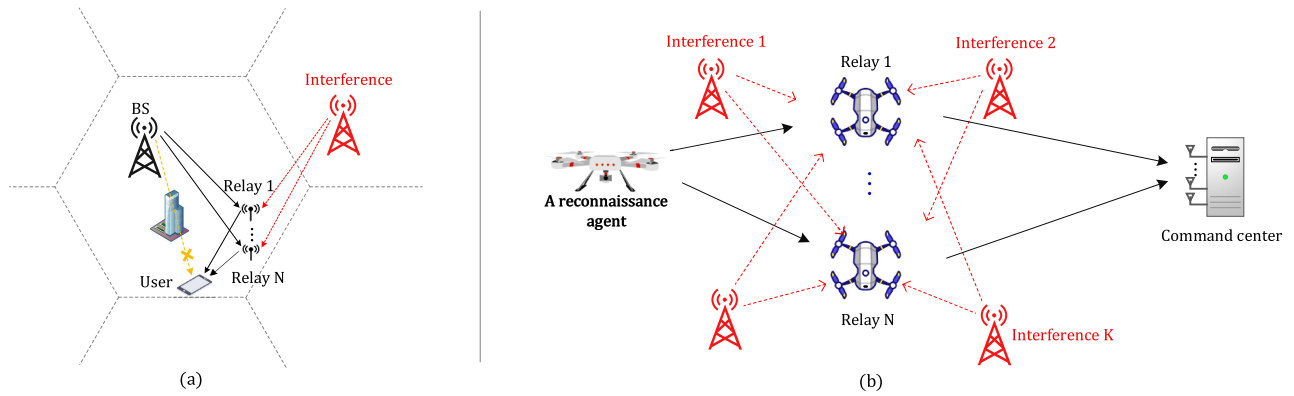


Fig. 1. Scenarios of relay communications under interferences.

the authors considered a relay network interfered by a jammer. But they assumed that a central processing unit can aggregate the received signals of the relays and the destination [18], which is usually too costly to be practical.

Categorized by the relay's operations, three types of relay schemes have been proposed, i.e., the compress-and-forward (CF) scheme [19], the decode-and-forward (DF) scheme [19], [20], and the amplify-and-forward (AF) scheme [11], [17], [20], among which the AF is particularly popular because it is simple-to-implement and has decent performance [11]–[13], [17], [21], [22]. Within the category of the AF scheme, some works take into account the nonlinearity of the power amplifier (PA).¹ This subcategory of work can be referred to as nonlinear amplify and forward (NAF) schemes, among which the authors in [23]–[27] only considered nonlinear PA at the relay node, and the authors in [28], [29] considered nonlinear PAs at both the source and the relay nodes. But they focused on analyzing the impact of the nonlinear PAs on the system performance rather than optimizing the relay network under the constraint of nonlinear PAs [28], [29]. Moreover, these NAF works are limited to the single-antenna source node.

B. Contributions

This paper aims at solving the following problem: Given M pairs of source and destination nodes that are wirelessly connected via N relays, how to coordinate these distributed multi-antenna nodes to avoid and suppress interference both internal and external of the network so that all the source nodes can communicate with their respective destination nodes, even without knowing the channel state information (CSI)?

To solve this problem, we present a novel perspective of relating a relay network to an artificial neural network (ANN) by drawing some striking similarities between them. Based on this perspective, we use the key technique of the backpropagation (BP) algorithm for an ANN [30], i.e., the chain rule of derivative, and propose a so-called distributed learning-based relay beamforming (DLRB) scheme to optimize the nonlinear transceivers

¹Although the nonlinearity is often ignored in the literature, it should never be ignored in practice for a non-constant modulus signal. Or the signal needs to be power backoff-ed to avoid distortion, but at the cost of output SNR and energy efficiency.

of the relay network, including the processing functions of the destinations, the relays, and the sources. The major contributions are summarized as follows:

- We introduce a novel perspective of relating a relay network to a neural network and thus borrow the idea of BP algorithm to train (optimize) the relay network.
- The proposed scheme can coordinate multiple relay nodes to form a virtual array for interference suppression, assuming no aggregation of data or CSI by a central unit.
- We show that imposing the *instantaneous* amplitude constraints of the sources and the relay nodes is not only practical, but also convenient in that it converts the original problem into an unconstrained optimization problem.
- We design a frame structure that enables the proposed DLRB scheme to track the time-varying channel with only a moderate training overhead.
- If the global CSI is known, the DLRB algorithm can also be implemented in a centralized way to optimize the nonlinear transceivers of the nodes via Monte Carlo simulations of the network rather than the over-the-air transmission of the training sequences.

While a relay network has many similarities to an ANN, they also differ in multiple aspects as will be discussed later in this paper. Hence, the relay network can be regarded as a “quasi-neural network,” a concept which we hope can find its use in other applications, since its topology allows for distributed optimization of the network.

The effectiveness of the proposed DLRB scheme has been verified by extensive simulations.

C. Organization

The rest of the paper is organized as follows. Section II introduces the single-user single-relay system model, formulates the problem, and draws the analogies between the relay network and an ANN. Section III proposes the DLRB algorithm, presents a frame design to support the DLRB algorithm, and introduces the centralized implementation. Section IV applies the DLRB algorithm to the multi-relay and multiuser scenarios and analyzes the complexity of the DLRB algorithm. Section V presents simulation results to verify the superior performance of the proposed algorithms over the state-of-the-art. Section VI gives the conclusion.

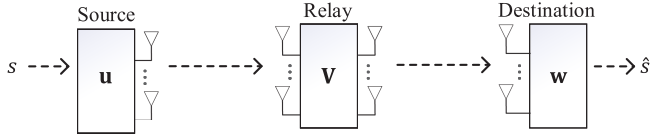


Fig. 2. A relay network with one source and destination ($M = 1$) and one relay ($N = 1$).

D. Notations

The following notations are used throughout this paper. $(\cdot)^*$, $(\cdot)^T$, and $(\cdot)^H$ stand for conjugate, transpose, and conjugate transpose, respectively. \mathbb{Z} is the set of integers. $\mathbb{C}^{N \times K}$ is the set of $N \times K$ complex matrices. $\sigma \circ \mathbf{V}$ stands for a composite function of $\sigma(\cdot)$ and \mathbf{V} . $\text{diag}(\mathbf{a})$ denotes a diagonal matrix with vector \mathbf{a} being its diagonal and $\text{vec}(\cdot)$ denotes a vectorization operation of stacking the columns of the matrix into a long column-vector. $|\mathbf{a}|$ stands for taking absolute value of \mathbf{a} element-wise and $\mathbf{a} \leq \mathbf{b}$ stands for $a_i \leq b_i$ element-wisely.

II. SYSTEM MODEL AND PROBLEM FORMULATION

A. System Model

We first consider the relay network as shown in Fig. 2, which consists of one M_s -antenna source, one M_r -input M_r -output relay node, and one M_d -antenna destination. The general case of multi-relay ($N \geq 2$) and multi-user ($M \geq 2$) will be discussed in Section IV.

The source wants to transmit a single stream $\{s(i), i \in \mathbb{Z}\}$ via the relay node to the destination. We assume that there is no direct link between the source and the destination.

Before transmitting signal s , the source processes it as

$$\mathbf{x} = f_s(s), \quad (1)$$

where $f_s: \mathbb{C} \rightarrow \mathbb{C}^{M_s}$, which we refer to as the processing function of the source, generates the signal being transmitted from the antenna array. The time index i is omitted for notational simplicity.

The relay node then receives

$$\mathbf{r} = \mathbf{H}_r \mathbf{x} + \boldsymbol{\eta}_r, \quad (2)$$

where $\mathbf{H}_r \in \mathbb{C}^{M_r \times M_s}$ represents the source-to-relay channel, which is frequency flat, and $\boldsymbol{\eta}_r \sim \mathcal{CN}(0, \sigma_r^2 \mathbf{I})$ is the noise.

To avoid self-interference, the relay node works in a frequency division duplex (FDD) mode, i.e., to receive and transmit on two different frequencies. Using $f_r: \mathbb{C}^{M_r} \rightarrow \mathbb{C}^{M_r}$ as its processing function, the relay transmits

$$\mathbf{a} = f_r(\mathbf{r}) \in \mathbb{C}^{M_r}. \quad (3)$$

The destination receives

$$\mathbf{y} = \mathbf{H}_d \mathbf{a} + \boldsymbol{\eta}_d, \quad (4)$$

where $\mathbf{H}_d \in \mathbb{C}^{M_d \times M_r}$ is the relay-to-destination channel, and $\boldsymbol{\eta}_d \sim \mathcal{CN}(0, \sigma_d^2 \mathbf{I})$ is the noise.

Applying the processing function $f_d: \mathbb{C}^{M_d} \rightarrow \mathbb{C}$ to the received signal, the destination yields

$$\hat{s} = f_d(\mathbf{y}). \quad (5)$$

These processing functions $f_s(\cdot)$, $f_r(\cdot)$, and $f_d(\cdot)$ are the transmit and receive functionalities of the nodes; thus, we also refer to them as the transceivers of the relay network.

B. Problem Formulation

This paper focuses on optimizing the transceivers of the nodes by the minimum mean squared error (MMSE) criterion subject to the *instantaneous* amplitude/power constraint *per antenna*, i.e.,

$$\begin{aligned} \min_{f_s(\cdot), f_r(\cdot), f_d(\cdot)} \quad & \mathbb{E} |\hat{s} - s|^2 \\ \text{s.t.} \quad & |\mathbf{x}| \leq \mathbf{1}, |\mathbf{a}| \leq \mathbf{1}, \end{aligned} \quad (6)$$

where \mathbf{x} and \mathbf{a} are given in (1) and (3), respectively, and to set the amplitude limit be 1 entails no loss of generality.

About the processing functions $f_s(\cdot)$ and $f_r(\cdot)$, we first let the source and the relay beamform the signal with weights $\mathbf{u} \in \mathbb{C}^{M_s}$ and $\mathbf{V} \in \mathbb{C}^{M_r \times M_r}$ as

$$\mathbf{z} \triangleq \mathbf{u} \mathbf{s} \in \mathbb{C}^{M_s}, \quad (7)$$

and

$$\mathbf{b} \triangleq \mathbf{V}^H \mathbf{r} \in \mathbb{C}^{M_r}, \quad (8)$$

respectively, before applying the *nonlinear* Soft Envelop Limiter (SEL) function [31, eq. (38)]²

$$\sigma(x) \triangleq \begin{cases} x & |x| \leq 1 \\ e^{j\angle(x)} & |x| > 1, \end{cases} \quad (9)$$

to clip the signal for instantaneous power constraint; here $\angle(\cdot)$ stands for taking the phase of a variable. Thus, $f_s(s) = \sigma \circ \mathbf{u} \mathbf{s}$ and $f_r(\mathbf{r}) = \sigma \circ \mathbf{V} \mathbf{r}$.

There are other models of the transfer function of PA, such as [32][33, eq. (3.25)]

$$\sigma(x) = \frac{|x| e^{j\angle(x)}}{(1 + |x|^{2p})^{\frac{1}{2p}}}. \quad (10)$$

But even if the SEL is not a good approximation to the real transfer function of PAs, it can serve as a clipping function to reduce the peak-to-average power ratio (PAPR) of the transmit signal so that the signal will stay in the linear region of the PA. Therefore, to choose which type of transfer function of the PA will cause no fundamental difference to our study.

Hence the transmitted signals from the source and the relay node are

$$\mathbf{x} = \sigma(\mathbf{z}) = \sigma(\mathbf{u} \mathbf{s}), \quad (11)$$

and

$$\mathbf{a} = \sigma(\mathbf{b}) = \sigma(\mathbf{V}^H \mathbf{r}), \quad (12)$$

respectively, where the clipping $\sigma(\cdot)$ is applied element-wise to \mathbf{z} and \mathbf{b} . Thus, the processing functions of the source node

²Although it is an abuse of notation to use σ at the risk of causing confusion with the noise power, we adopt it to emphasize its connection to the activation function in ANN.

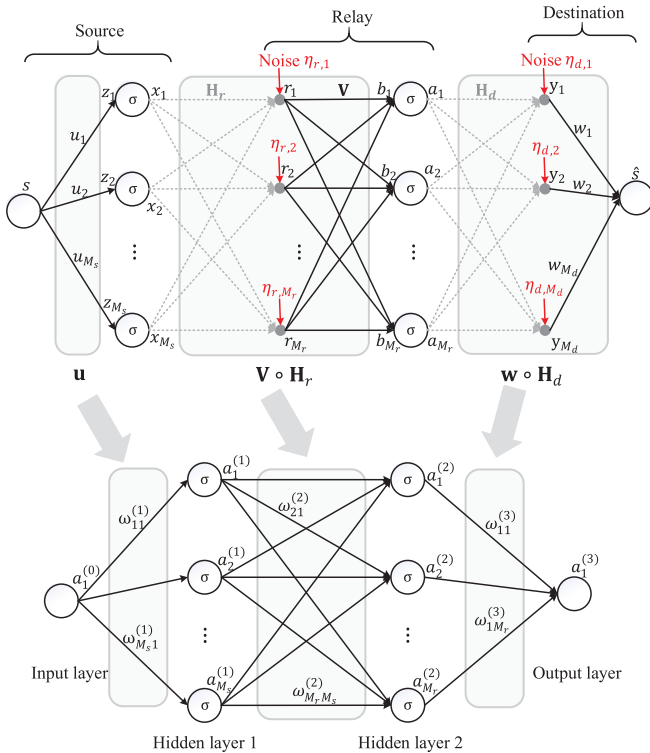


Fig. 3. A relay network shown in the upper subplot is analogous to a four-layer ANN shown in the lower subplot.

and the relay node, i.e., $f_s(s) = \sigma \circ \mathbf{u}s$ and $f_r(\mathbf{r}) = \sigma \circ \mathbf{V}\mathbf{r}$, are both nonlinear composite functions.

In the end, the destination node applies a linear beamformer $\mathbf{w} \in \mathbb{C}^{M_d}$ to obtain

$$\hat{s} = f_d(\mathbf{y}) = \mathbf{w}^H \mathbf{y} \in \mathbb{C}. \quad (13)$$

According to the signal transmission process, we obtain \mathbf{x} from (11), \mathbf{a} from (2) and (12), and then \hat{s} from (4) and (13). Inserting \hat{s} into the objection function in (6), we get a unconstrained problem

$$\min_{\mathbf{u}, \mathbf{V}, \mathbf{w}} \mathbb{E} |\mathbf{w}^H [\mathbf{H}_d \sigma(\mathbf{V}^H (\mathbf{H}_r \sigma(\mathbf{u}s) + \boldsymbol{\eta}_r)) + \boldsymbol{\eta}_d] - s|^2. \quad (14)$$

The instantaneous power constraint in (6) is omitted because it is automatically met by the nonlinear SEL $\sigma(\cdot)$ in (11) and (12).

To optimize (14) appears challenging because i) the SEL $\sigma(\cdot)$ is nonlinear and ii) the closed-form expression of the expectation appears intractable. Its distributed optimization appears even more difficult. The key is to relate a relay network to an ANN and hence to borrow the idea of the BP algorithm to propose a distributed learning method for optimizing the relay network.

C. The Analogies Between a Relay Network and an ANN

We present the diagram of the relay network in the upper subplot of Fig. 3, and observe its striking analogies to the ANN shown in the lower subplot, which are as follows:

- i) the antennas of the source, the relay, and the destination are analogous to the neurons in the different layers of the ANN;
- ii) the data transmission from the source node to the relay node and then to the destination is like the propagation of the training data between the layers in the ANN;
- iii) the operations \mathbf{u} , $\mathbf{V} \circ \mathbf{H}_r$, and $\mathbf{w} \circ \mathbf{H}_d$ in the relay network are analogous to the connection weights $\omega^{(l)}$, $l = 1, 2, 3$ in the four-layer ANN, respectively, as illustrated by the gray rectangles in Fig. 3;
- iv) the SEL $\sigma(\cdot)$ of the source and the relay is analogous to the activation function of the hidden layer 1 and hidden layer 2 in ANN, although the latter typically uses a Sigmoid function or a Rectified Linear Unit (ReLU).

There are, however, key differences between the ANN and relay networks:

- i) in an ANN the data are being exchanged in an error-free manner; but in the relay network the signal will be contaminated by channel noise/interferences as shown in the upper subplot of Fig. 3;
- ii) in an ANN all the connection weights are known and adjustable, whereas in the relay network the “connection weights” include the wireless channels, which are unknown and can not be adjusted;
- iii) all data and parameters in an ANN are real, while in the relay network they are complex-valued.

Given the similarities and differences between a relay network and an ANN, we refer to a relay network as a *quasi-neural network*. Since the connection weights in an ANN can be effectively optimized using the BP algorithm, one can conjecture that the relay network may be similarly optimized. Indeed, we will show in the next how the relay network can be optimized in a distributed manner using the chain rule of derivative, which is also the key to the BP.

III. THE DISTRIBUTED LEARNING-BASED RELAY BEAMFORMING (DLRB) SCHEME

In this section, we assume that the CSI is static but unknown, and propose the DLRB scheme that can solve (14) based on pilot sequences.

A. The DLRB Algorithm

Considering

$$J \triangleq |\hat{s} - s|^2 \quad (15)$$

as a single realization of the cost function of (14), we attempt to minimize J with respect to the weights of the source, the relay, and the destination. To this end, we derive the gradients $\frac{\partial J}{\partial \mathbf{u}^*}$, $\frac{\partial J}{\partial \mathbf{V}^*}$, and $\frac{\partial J}{\partial \mathbf{w}^*}$ based on a single sample of the pilot $s(i)$. Inspired by the BP algorithm, we use the chain rule of derivatives to establish the following proposition.

Proposition III.1: The derivative with respect to the weight of the destination is

$$\frac{\partial J}{\partial \mathbf{w}^*} = \mathbf{y} \left(\frac{\partial J}{\partial \hat{s}^*} \right)^*, \quad (16)$$

where

$$\frac{\partial J}{\partial \hat{s}^*} = \hat{s} - s. \quad (17)$$

The derivative with respect to the weight of the relay is

$$\frac{\partial J}{\partial \mathbf{V}^*} = \mathbf{r} \left(\frac{\partial J}{\partial \mathbf{b}^*} \right)^H, \quad (18)$$

where

$$\frac{\partial J}{\partial \mathbf{b}^*} = \frac{\partial \mathbf{a}^*}{\partial \mathbf{b}^*} \frac{\partial J}{\partial \mathbf{a}^*} + \frac{\partial \mathbf{a}}{\partial \mathbf{b}^*} \left(\frac{\partial J}{\partial \mathbf{a}^*} \right)^*, \quad (19)$$

$$\frac{\partial J}{\partial \mathbf{a}^*} = \mathbf{H}_d^H \mathbf{w} \frac{\partial J}{\partial \hat{s}^*}, \quad (20)$$

$$\frac{\partial \mathbf{a}^*}{\partial \mathbf{b}^*} = \text{diag} \left(\frac{\partial a_1^*}{\partial b_1^*}, \dots, \frac{\partial a_{M_r}^*}{\partial b_{M_r}^*} \right), \quad (21)$$

and

$$\frac{\partial \mathbf{a}}{\partial \mathbf{b}^*} = \text{diag} \left(\frac{\partial a_1}{\partial b_1^*}, \dots, \frac{\partial a_{M_r}}{\partial b_{M_r}^*} \right), \quad (22)$$

with

$$\frac{\partial a_q^*}{\partial b_q^*} = \begin{cases} 1 & |b_q| \leq 1 \\ \frac{1}{2|b_q|} & |b_q| > 1 \end{cases}, \quad q = 1, \dots, M_r, \quad (23)$$

and³

$$\frac{\partial a_q}{\partial b_q^*} = \begin{cases} 0 & |b_q| \leq 1 \\ -\frac{1}{2|b_q|} e^{j2\angle(b_q)} & |b_q| > 1 \end{cases}, \quad q = 1, \dots, M_r. \quad (24)$$

The derivative with respect to the weight of the source is

$$\frac{\partial J}{\partial \mathbf{u}^*} = s^* \left(\frac{\partial J}{\partial \mathbf{z}^*} \right), \quad (25)$$

where

$$\frac{\partial J}{\partial \mathbf{z}^*} = \frac{\partial \mathbf{x}^*}{\partial \mathbf{z}^*} \frac{\partial J}{\partial \mathbf{x}^*} + \frac{\partial \mathbf{x}}{\partial \mathbf{z}^*} \left(\frac{\partial J}{\partial \mathbf{x}^*} \right)^*, \quad (26)$$

$$\frac{\partial J}{\partial \mathbf{x}^*} = \mathbf{H}_r^H \mathbf{V} \frac{\partial J}{\partial \mathbf{b}^*}, \quad (27)$$

$$\frac{\partial \mathbf{x}^*}{\partial \mathbf{z}^*} = \text{diag} \left(\frac{\partial x_1^*}{\partial z_1^*}, \dots, \frac{\partial x_{M_s}^*}{\partial z_{M_s}^*} \right), \quad (28)$$

and

$$\frac{\partial \mathbf{x}}{\partial \mathbf{z}^*} = \text{diag} \left(\frac{\partial x_1}{\partial z_1^*}, \dots, \frac{\partial x_{M_s}}{\partial z_{M_s}^*} \right), \quad (29)$$

with

$$\frac{\partial x_p^*}{\partial z_p^*} = \begin{cases} 1 & |z_p| \leq 1 \\ \frac{1}{2|z_p|} & |z_p| > 1 \end{cases}, \quad p = 1, \dots, M_s, \quad (30)$$

and

$$\frac{\partial x_p}{\partial z_p^*} = \begin{cases} 0 & |z_p| \leq 1 \\ -\frac{1}{2|z_p|} e^{j2\angle(z_p)} & |z_p| > 1 \end{cases}, \quad p = 1, \dots, M_s. \quad (31)$$

³Note that $\frac{\partial a_q^*}{\partial b_q^*} \neq \left(\frac{\partial a_q}{\partial b_q^*} \right)^*$.

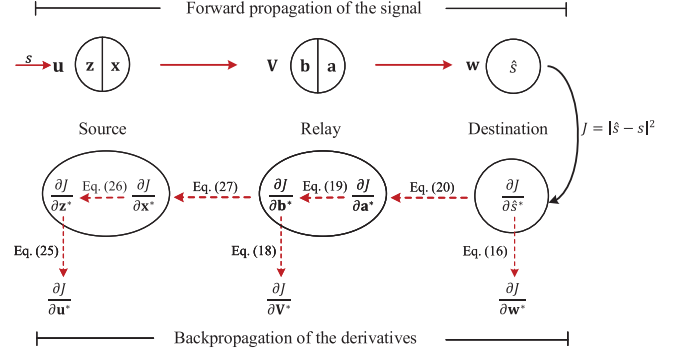


Fig. 4. The schematic diagram of the DLRB algorithm consisting of the forward propagation of the signal and the back-propagation of the derivatives.

Proof: The proof is relegated to Appendix.

Based on Proposition III.1, all the distributed nodes can update their processing weights based on the derivatives (16), (18) and (25). Indeed, combining (16) and (17) yields $\frac{\partial J}{\partial \mathbf{w}^*} = \mathbf{y}(\hat{s} - s)^*$; thus, the destination node can update \mathbf{w} using \mathbf{y} and \hat{s} , which are both locally available given known pilot s . Therefore, the destination can update its weight without the CSI.

Combining (18) (19) and (20) yields

$$\frac{\partial J}{\partial \mathbf{V}^*} = \mathbf{r} \left[\frac{\partial \mathbf{a}^*}{\partial \mathbf{b}^*} \left(\mathbf{H}_d^H \mathbf{w} \frac{\partial J}{\partial \hat{s}^*} \right) + \frac{\partial \mathbf{a}}{\partial \mathbf{b}^*} \left(\mathbf{H}_d^H \mathbf{w} \frac{\partial J}{\partial \hat{s}^*} \right)^* \right]^H. \quad (32)$$

Note that \mathbf{r} and $\frac{\partial \mathbf{a}}{\partial \mathbf{b}^*}$, $\frac{\partial \mathbf{a}^*}{\partial \mathbf{b}^*}$ are all locally available to the relay node [cf. (21)-(24)]. Let the destination broadcast the beamformed derivative $(\mathbf{w} \frac{\partial J}{\partial \hat{s}^*})^*$ to the relay node through the reverse channel. Owing to the channel reciprocity, the relay will receive the signal $\mathbf{H}_d^T (\mathbf{w} \frac{\partial J}{\partial \hat{s}^*})^* = (\frac{\partial J}{\partial \mathbf{a}^*})^*$. Therefore, the relay can obtain the derivative (32) without knowing the CSI, given the reverse communication link from the destination to the relay.

The source node can obtain the derivative in (25) in a way similar to the relay node's obtaining (18). Combining (25), (26), and (27) yields

$$\frac{\partial J}{\partial \mathbf{u}^*} = s^* \left[\frac{\partial \mathbf{x}^*}{\partial \mathbf{z}^*} \left(\mathbf{H}_r^H \mathbf{V} \frac{\partial J}{\partial \mathbf{b}^*} \right) + \frac{\partial \mathbf{x}}{\partial \mathbf{z}^*} \left(\mathbf{H}_r^H \mathbf{V} \frac{\partial J}{\partial \mathbf{b}^*} \right)^* \right]. \quad (33)$$

Note that s^* , $\frac{\partial \mathbf{x}}{\partial \mathbf{z}^*}$, and $\frac{\partial \mathbf{x}^*}{\partial \mathbf{z}^*}$ are locally available [cf. (28)–(31)]. Let the relay node broadcast the beamformed derivative $(\mathbf{V} \frac{\partial J}{\partial \mathbf{b}^*})^*$ to the source node through the reverse channel. Owing to the channel reciprocity, the source will receive the signal $\mathbf{H}_r^T (\mathbf{V} \frac{\partial J}{\partial \mathbf{b}^*})^*$. Therefore, the source can obtain the derivative (33) without knowing the CSI, given the reverse communication link from the relay to the source.

Now we see that the distributed nodes obtain the derivatives of their respective weights through two phases as shown in Fig. 4: the forward propagation of the signal, and the backpropagation of the derivatives. In Phase I, the source transmits the beamformed signal $\sigma(\mathbf{u}s)$, the relay forwards the received signal $\sigma(\mathbf{V}^H \mathbf{r})$, and the destination applies an equalizer to the received vector \mathbf{y} to obtain $\hat{s} = \mathbf{w}^H \mathbf{y}$; In Phase II, the destination node transmits the beamformed derivative $(\mathbf{w} \frac{\partial J}{\partial \hat{s}^*})^*$ to the relay node, and the relay node receives $(\frac{\partial J}{\partial \mathbf{a}^*})^*$ as shown in (20) and transmits

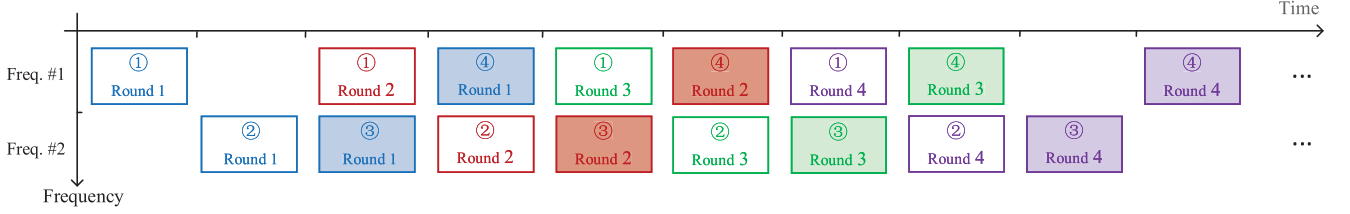
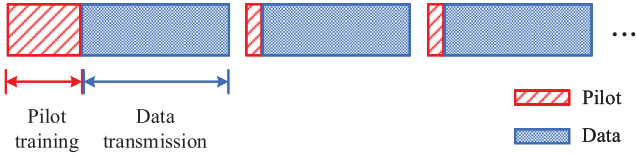
Fig. 6. T rounds of the forward and backward training sessions.

Fig. 7. Schematic diagram of the pilot-data alternating process of a relay network using the DLRB algorithm.

As shown in Fig. 4, the DLRB algorithm transfers information in both forward and backward directions. The forward signal propagation in Fig. 4 corresponds to the source-to-relay and the relay-to-destination transmission, which is shown by ① and ② in Fig. 5; and the back-propagation in Fig. 4 corresponds to the destination-to-relay and the relay-to-source transmission, which is shown by ③ and ④ in Fig. 5.

To support the forward and backward transmission needed in the DLRB algorithm, we design the frame that contains the periodic pilots and the time slots as shown in Fig. 6. The time gaps between the T rounds of the forward and backward training sessions are to accommodate for the over-the-air propagation delay and the processing time.

In summary, the DLRB scheme is conducted *over-the-air*: it has the source transmit the pilot sequences processed by $\sigma \circ \mathbf{u}$; it has the relay forward the received samples being processed by $\sigma \circ \mathbf{V}$; and it has the destination and the relay node broadcast the beamformed derivatives, i.e., $(\mathbf{w} \frac{\partial J}{\partial \mathbf{s}^*})^*$ and $(\mathbf{V} \frac{\partial J}{\partial \mathbf{b}^*})^*$ in the back-propagation channel. Each node can obtain the required derivatives, and then update the weights.

After the initial T rounds of the over-the-air training in Fig. 6, the users can transmit their payload data. Following the preamble is the data payload as shown in Fig. 7. When the wireless channels are time-varying, we need to retrain the relay network every once in a while. But the subsequent trainings will take significantly fewer training iterations since they are warm-started. The pilot-data alternating process is shown in Fig. 7, where the training session after the initial one is significantly briefer.

C. The Centralized Implementation

If the CSI \mathbf{H}_r and \mathbf{H}_d are globally known at some central unit, it can implement the DLRB algorithm in a processor rather than using the over-the-air training.

The cost function in (14) can be expanded as

$$\begin{aligned} \check{J} \triangleq & \mathbf{w}^H (\mathbf{H}_d \mathbb{E}[\mathbf{a}\mathbf{a}^H] \mathbf{H}_d^H + \sigma_d^2 \mathbf{I}) \mathbf{w} - \mathbb{E}[\mathbf{s}\mathbf{a}^H] \mathbf{H}_d^H \mathbf{w} \\ & - \mathbf{w}^H \mathbf{H}_d \mathbb{E}[\mathbf{a}\mathbf{s}^*] + \mathbb{E}[\mathbf{s}^* \mathbf{s}], \end{aligned} \quad (43)$$

where the cross term of the signal and the noise has been discarded.

Note that $\check{J} = \mathbb{E}[J]$. Hence the derivative of \check{J} with respect to the destination's weight is

$$\frac{\partial \check{J}}{\partial \mathbf{w}^*} = (\mathbf{H}_d \mathbb{E}[\mathbf{a}\mathbf{a}^H] \mathbf{H}_d^H + \sigma_d^2 \mathbf{I}) \mathbf{w} - \mathbf{H}_d \mathbb{E}[\mathbf{a}\mathbf{s}^*] \quad (44)$$

$$= \mathbb{E} \left[\frac{\partial J}{\partial \mathbf{w}^*} \right], \quad (45)$$

i.e., it is the expectation of (16). Although $\mathbb{E}[\mathbf{a}\mathbf{a}^H]$ and $\mathbb{E}[\mathbf{a}\mathbf{s}^*]$ are difficult to obtain analytically owing to the nonlinear function $\sigma(\cdot)$, we can use Monte Carlo trials to approximate them as

$$\mathbb{E}[\mathbf{a}\mathbf{a}^H] \approx \frac{1}{L} \sum_{i=1}^L \mathbf{a}(i)\mathbf{a}(i)^H, \quad (46)$$

and

$$\mathbb{E}[\mathbf{a}\mathbf{s}^*] \approx \frac{1}{L} \sum_{i=1}^L \mathbf{a}(i)s(i)^*. \quad (47)$$

Similarly, $\frac{\partial \check{J}}{\partial \mathbf{V}^*} = \mathbb{E}[\frac{\partial J}{\partial \mathbf{V}^*}]$, i.e., it is the expectation of (18). It follows from (18) that we can approximate it using Monte Carlo trials

$$\frac{\partial \check{J}}{\partial \mathbf{V}^*} \approx \frac{1}{L} \sum_{i=1}^L \mathbf{r}(i)\boldsymbol{\psi}(i)^H, \quad (48)$$

where $\boldsymbol{\psi}(i) = \frac{\partial \mathbf{a}^*}{\partial \mathbf{b}^*}(i)\phi(i) + \frac{\partial \mathbf{a}}{\partial \mathbf{b}^*}(i)\phi(i)^*$ with $\phi(i) = \mathbf{H}_d^H \mathbf{w} [\mathbf{w}^H \mathbf{H}_d \mathbf{a}(i) - s(i)]$.

According to (25), we can obtain

$$\begin{aligned} \frac{\partial \check{J}}{\partial \mathbf{u}^*} \approx & \frac{1}{L} \sum_{i=1}^L s(i)^* \left\{ \frac{\partial \mathbf{x}^*}{\partial \mathbf{z}^*}(i) [\mathbf{H}_r^H \mathbf{V} \boldsymbol{\psi}(i)] \right. \\ & \left. + \frac{\partial \mathbf{x}}{\partial \mathbf{z}^*}(i) [\mathbf{H}_r^H \mathbf{V} \boldsymbol{\psi}(i)]^* \right\}. \end{aligned} \quad (49)$$

Using the derivatives in (44), (48) and (49) instead of $\bar{\mathbf{d}}_{\mathbf{w}}$, $\bar{\mathbf{d}}_{\mathbf{V}}$, and $\bar{\mathbf{d}}_{\mathbf{u}}$ in (37)-(39), we can update \mathbf{u} , \mathbf{V} , and \mathbf{w} according to (40)-(42).

IV. EXTENSION OF THE DLRB ALGORITHM TO MULTI-RELAY AND MULTI-USER SCENARIOS

This section considers the multi-relay and multi-user cases as shown in Fig. 8 and Fig. 9, respectively. Next, we will show how the DLRB algorithm can be generalized for the two scenarios.

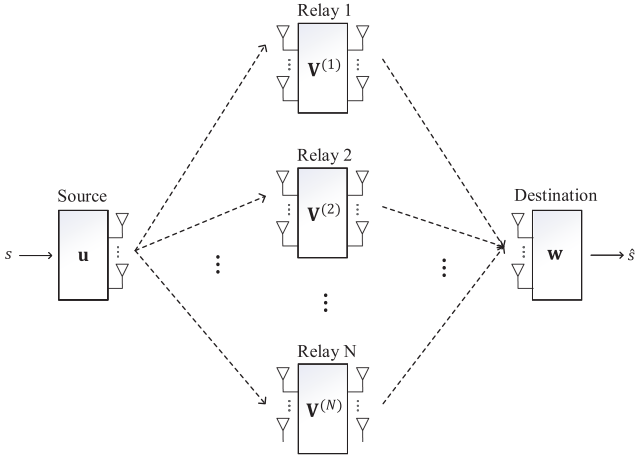


Fig. 8. A multi-relay network.

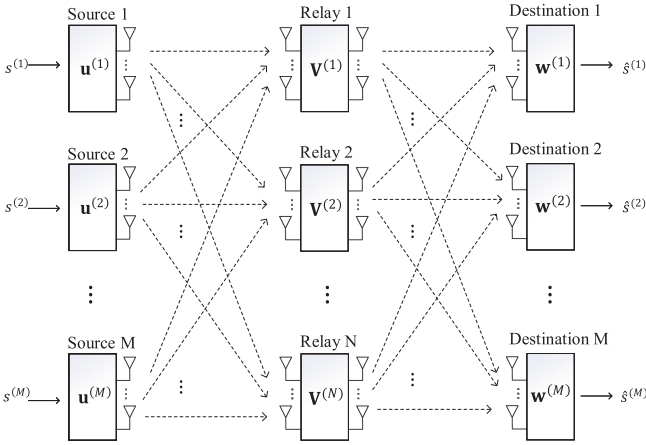


Fig. 9. A multi-user relay network.

A. The Multi-Relay Scenario

Given N relay nodes as shown in Fig. 8, of which the n -th receives

$$\mathbf{r}^{(n)} = \mathbf{H}_r^{(n)} \mathbf{x} + \boldsymbol{\eta}_r^{(n)}, \quad n = 1, \dots, N, \quad (50)$$

where \mathbf{x} is shown in (11), $\mathbf{H}_r^{(n)} \in \mathbb{C}^{M_r \times M_s}$ represents the channel between the source and the n -th relay, and $\boldsymbol{\eta}_r^{(n)} \sim \mathcal{CN}(0, \sigma_r^2 \mathbf{I})$ is the noise.

Being consistent with the single-relay case as shown in (12), the n -th relay applies the weight $\mathbf{V}^{(n)} \in \mathbb{C}^{M_r \times M_r}$ and the nonlinear processing $\sigma(\cdot)$ to obtain

$$\mathbf{b}^{(n)} = \mathbf{V}^{(n)H} \mathbf{r}^{(n)}, \quad (51)$$

and

$$\mathbf{a}^{(n)} = \sigma(\mathbf{b}^{(n)}). \quad (52)$$

Denote

$$\tilde{\mathbf{a}} \triangleq \text{vec}([\mathbf{a}^{(1)}, \mathbf{a}^{(2)}, \dots, \mathbf{a}^{(N)}]) \in \mathbb{C}^{NM_r}. \quad (53)$$

The destination receives $\mathbf{y} = \mathbf{H}_d \tilde{\mathbf{a}} + \boldsymbol{\eta}_d$ and obtains the estimated signal $\hat{s} = \mathbf{w}^H \mathbf{y}$, which are consistent with (4) and (13), respectively. Accordingly, the derivative is the same as (16)-(17),

i.e.,

$$\frac{\partial J}{\partial \mathbf{w}^*} = \mathbf{y} \left(\frac{\partial J}{\partial \hat{s}^*} \right)^* = \mathbf{y} (\hat{s} - s)^*. \quad (54)$$

Here we assume that the clocks of the relay nodes are synchronized and thus $\mathbf{a}^{(n)}$'s are time-aligned [34], [35].

According to (51) and (52), the signal processing for each relay here is the same as that in a single-relay scenario [cf. (12)]. Therefore, the derivatives with respect to the n -th relay's parameters are the same as defined in (18)-(24) except for adding the superscript (n) , i.e.,

$$\begin{aligned} \frac{\partial J}{\partial \mathbf{V}^{(n)*}} &= \mathbf{r}^{(n)} \left[\frac{\partial \mathbf{a}^{(n)*}}{\partial \mathbf{b}^{(n)*}} \left(\mathbf{H}_d^{(n)H} \mathbf{w} \frac{\partial J}{\partial \hat{s}^*} \right) \right. \\ &\quad \left. + \frac{\partial \mathbf{a}^{(n)}}{\partial \mathbf{b}^{(n)*}} \left(\mathbf{H}_d^{(n)H} \mathbf{w} \frac{\partial J}{\partial \hat{s}^*} \right)^* \right]^H, \end{aligned} \quad (55)$$

where $\mathbf{H}_d^{(n)} \in \mathbb{C}^{M_d \times M_r}$ is the channel between the n -th relay and the destination.

The signal processing for each user here is also the same as that in a single-relay scenario, as shown in (11). Accordingly, the derivatives are the same as defined in (25)-(31), except that (27) becomes a superimposed term due to the presence of multiple relay nodes, i.e.,

$$\frac{\partial J}{\partial \mathbf{u}^*} = s^* \left(\frac{\partial J}{\partial \mathbf{z}^*} \right) = s^* \left(\frac{\partial \mathbf{x}^*}{\partial \mathbf{z}^*} \frac{\partial J}{\partial \mathbf{x}^*} + \frac{\partial \mathbf{x}}{\partial \mathbf{z}^*} \frac{\partial J}{\partial \mathbf{x}} \right), \quad (56)$$

with

$$\frac{\partial J}{\partial \mathbf{x}^*} = \sum_{n=1}^N \mathbf{H}_r^{(n)H} \mathbf{V}^{(n)} \frac{\partial J}{\partial \mathbf{b}^{(n)*}}. \quad (57)$$

According to (54), the destination node can update its weight \mathbf{w} using the local information \mathbf{y} , \hat{s} , and s ; according to (55), given that the destination broadcasts $\mathbf{w} \frac{\partial J}{\partial \hat{s}^*}$ in the reverse channel, all the relay nodes can receive $\mathbf{H}_d^{(n)T} (\mathbf{w} \frac{\partial J}{\partial \hat{s}^*})^*$, $n = 1, \dots, N$ respectively, and then obtain their own derivatives $\frac{\partial J}{\partial \mathbf{V}^{(n)*}}$, $n = 1, \dots, N$. According to (56)-(57), we see that given that all the N relay nodes transmit $\mathbf{V}^{(n)} \frac{\partial J}{\partial \mathbf{b}^{(n)*}}$, $n = 1, \dots, N$ in a time-aligned manner, the source node will receive the superimposed term $\sum_{n=1}^N \mathbf{H}_r^{(n)H} \mathbf{V}^{(n)} \frac{\partial J}{\partial \mathbf{b}^{(n)*}}$ and thus can obtain the derivative $\frac{\partial J}{\partial \mathbf{u}^*}$.

Therefore, the DLRB algorithm can optimize the multi-relay network using no explicit channel information, nor information exchange between the distributed relay nodes.

Moreover, the DLRB algorithm can achieve the MMSE solution in the presence of interferences even without knowing the directions of the interferences. In other words, the relay nodes are being coordinated by the destination nodes to form a virtual array for interference suppression but with no CSI and no information exchange among themselves.

Given enough training plots, one can achieve accurate estimation of the source-to-relay channels and relay-to-destination channels. The interferences, however, are noncooperative; thus, their CSI is difficult to obtain, if ever possible. Therefore, it is difficult for a conventional channel-estimation-based relay beamforming approach to achieve interference suppression

without the interference's CSI. In contrast, our DLRB scheme can coordinate the distributed relay nodes to mitigate the interferences, requiring neither the interference CSI nor information exchange between the relays, which is a unique advantage of this work.

B. The Multiuser Scenario

Now we consider a relay network containing M pairs of users, i.e., M sources and M corresponding destinations as shown in Fig. 9. The m -th source applies the weight $\mathbf{u}^{(m)} \in \mathbb{C}^{M_s}$ and the nonlinear processing $\sigma(\cdot)$ to the signal $s^{(m)}$ as

$$\mathbf{x}^{(m)} = \sigma(\mathbf{z}^{(m)}) = \sigma(\mathbf{u}^{(m)} s^{(m)}), \quad m = 1, 2, \dots, M. \quad (58)$$

Denote $\tilde{\mathbf{x}} \triangleq \text{vec}([\mathbf{x}^{(1)}, \mathbf{x}^{(2)}, \dots, \mathbf{x}^{(M)}]) \in \mathbb{C}^{MM_s}$. The n -th relay receives

$$\mathbf{r}^{(n)} = \tilde{\mathbf{H}}_r^{(n)} \tilde{\mathbf{x}} + \boldsymbol{\eta}_r^{(n)}, \quad (59)$$

where $\tilde{\mathbf{H}}_r^{(n)} \in \mathbb{C}^{M_r \times MM_s}$ represents the channel between all M sources and the n -th relay.

After the relay processes its received signal according to (51)-(53), the destination receives

$$\mathbf{y}^{(m)} = \mathbf{H}_d^{(m)} \tilde{\mathbf{a}} + \boldsymbol{\eta}_d^{(m)}, \quad (60)$$

where $\mathbf{H}_d^{(m)} \in \mathbb{C}^{M_d \times NM_r}$ represents the channel between all N relays and the m -th destination. Applying the linear beamformer $\mathbf{w}^{(m)} \in \mathbb{C}^{M_d}$ to the received signal, the m -th destination yields

$$\hat{s}^{(m)} = \mathbf{w}^{(m)H} \mathbf{y}^{(m)}. \quad (61)$$

Similar to the single-user case [cf. (15)], we attempt to minimize

$$J \triangleq \sum_{m=1}^M |\hat{s}^{(m)} - s^{(m)}|^2. \quad (62)$$

Being consistent with (54), (55), and (56), the derivative with respect to the m -th destination's weight is

$$\frac{\partial J}{\partial \mathbf{w}^{(m)*}} = \mathbf{y}^{(m)} \left(\frac{\partial J}{\partial \hat{s}^{(m)*}} \right)^* = \mathbf{y}^{(m)} (\hat{s}^{(m)} - s^{(m)})^*; \quad (63)$$

the derivative with respect to the n -th relay's weight is

$$\begin{aligned} \frac{\partial J}{\partial \mathbf{V}^{(n)*}} &= \mathbf{r}^{(n)} \left\{ \frac{\partial \mathbf{a}^{(n)*}}{\partial \mathbf{b}^{(n)*}} \left[\sum_{m=1}^M \mathbf{H}_d^{(m,n)H} \left(\mathbf{w}^{(m)} \frac{\partial J}{\partial \hat{s}^{(m)*}} \right) \right] \right. \\ &\quad \left. + \frac{\partial \mathbf{a}^{(n)}}{\partial \mathbf{b}^{(n)*}} \left[\sum_{m=1}^M \mathbf{H}_d^{(m,n)H} \left(\mathbf{w}^{(m)} \frac{\partial J}{\partial \hat{s}^{(m)*}} \right) \right]^* \right\}^H, \end{aligned} \quad (64)$$

where $\mathbf{H}_d^{(m,n)}$ is the channel between the m -th destination and the n -th relay; and the derivative with respect to the m -th source's weight is

$$\frac{\partial J}{\partial \mathbf{u}^{(m)*}} = s^{(m)*} \left\{ \frac{\partial \mathbf{x}^{(m)*}}{\partial \mathbf{z}^{(m)*}} \left[\sum_{n=1}^N \mathbf{H}_r^{(n,m)H} \left(\mathbf{V}^{(n)} \frac{\partial J}{\partial \mathbf{b}^{(n)*}} \right) \right] \right\}$$

$$+ \frac{\partial \mathbf{x}^{(m)}}{\partial \mathbf{z}^{(m)*}} \left[\sum_{n=1}^N \mathbf{H}_r^{(n,m)H} \left(\mathbf{V}^{(n)} \frac{\partial J}{\partial \mathbf{b}^{(n)*}} \right) \right]^* \Bigg\}, \quad (65)$$

where $\mathbf{H}_r^{(n,m)}$ is the channel between the n -th relay and the m -th source.

According to (63), each destination node can obtain their own derivative $\frac{\partial J}{\partial \mathbf{w}^{(m)*}}$, $m = 1, 2, \dots, M$ using the received signal $\mathbf{y}^{(m)}$, the output signal \hat{s} , and the known pilot s . According to (64), if all the destinations broadcast $\mathbf{w}^{(m)} \frac{\partial J}{\partial \hat{s}^{(m)*}}$, $m = 1, 2, \dots, M$ to the relay nodes in a synchronized manner, then each relay will receive the superimposed term $\sum_{m=1}^M \mathbf{H}_d^{(m,n)H} \mathbf{w}^{(m)} \frac{\partial J}{\partial \hat{s}^{(m)*}}$ and thus obtain their own derivative $\frac{\partial J}{\partial \mathbf{V}^{(n)*}}$, $n = 1, 2, \dots, N$. According to (65), if the relay nodes broadcast $\mathbf{V}^{(n)} \frac{\partial J}{\partial \mathbf{b}^{(n)*}}$, $n = 1, 2, \dots, N$ to the sources in a synchronized manner, then each source will receive the superimposed term $\sum_{n=1}^N \mathbf{H}_r^{(n,m)H} \mathbf{V}^{(n)} \frac{\partial J}{\partial \mathbf{b}^{(n)*}}$ and thus obtain their own derivative $\frac{\partial J}{\partial \mathbf{u}^{(m)*}}$, $m = 1, 2, \dots, M$.

Therefore, the DLRB algorithm can optimize the multi-user relay network using no explicit channel information, and it requires no information exchange between the distributed relay/source/destination nodes.

C. Complexity Analysis

In the DLRB scheme, each node only needs to calculate the beamforming signal, i.e., $\mathbf{u}^{(m)} s^{(m)}$, $\mathbf{V}^{(n)H} \mathbf{r}^{(n)}$, or $\mathbf{w}^{(m)H} \mathbf{y}^{(m)}$ in forward propagation [cf. (58), (51), or (61)], and the derivative with respect to its own weight, i.e., $\frac{\partial J}{\partial \mathbf{u}^{(m)*}}$, $\frac{\partial J}{\partial \mathbf{V}^{(n)*}}$, or $\frac{\partial J}{\partial \mathbf{w}^{(m)*}}$ in the backpropagation [cf. (65), (64), or (63)].

On the destination side, according to (61), each destination node takes M_d multiplications to compute signal $\mathbf{w}^{(m)H} \mathbf{y}^{(m)}$ in the forward propagation; according to (63), the destination needs M_d multiplications to compute $\frac{\partial J}{\partial \mathbf{w}^{(m)*}}$ in the backpropagation. In addition, the destination requires M_d multiplications to compute $\mathbf{w}^{(m)} \frac{\partial J}{\partial \hat{s}^{(m)*}}$ to feed back to the relay in the reverse channel [cf. (64)]. As an L -length pilot is used for updating the weight each time, the destination performs a total of $3M_d L$ multiplications in each round of training.

On the relay side, according to (51), each relay node takes M_r^2 multiplications to compute beamforming signal $\mathbf{V}^{(n)H} \mathbf{r}^{(n)}$ in the forward propagation; according to (64), in the backpropagation the relay first needs $2M_r$ multiplications to compute $\frac{\partial \mathbf{a}^{(n)*}}{\partial \mathbf{b}^{(n)*}} \boldsymbol{\xi}_r^{(n)}$ and $\frac{\partial \mathbf{a}^{(n)}}{\partial \mathbf{b}^{(n)*}} \boldsymbol{\xi}_r^{(n)*}$, where $\boldsymbol{\xi}_r^{(n)} \triangleq \sum_{m=1}^M \mathbf{H}_d^{(m,n)H} \left(\mathbf{w}^{(m)} \frac{\partial J}{\partial \hat{s}^{(m)*}} \right)$ is the received feedback signal – note that the summations and matrix-vector multiplications are automatically conducted via the over-the-air propagation without calculation. Then the relay needs M_r^2 multiplications to multiply signal $\mathbf{r}^{(n)}$ with $(\frac{\partial \mathbf{a}^{(n)*}}{\partial \mathbf{b}^{(n)*}} \boldsymbol{\xi}_r^{(n)} + \frac{\partial \mathbf{a}^{(n)}}{\partial \mathbf{b}^{(n)*}} \boldsymbol{\xi}_r^{(n)*})^H$ to obtain $\frac{\partial J}{\partial \mathbf{V}^{(n)*}}$. In addition, the relay requires M_r^2 multiplications to compute $\mathbf{V}^{(n)} \frac{\partial J}{\partial \mathbf{b}^{(n)*}}$ before feeding it back to the source node [cf. (65)]. Therefore, the relay node performs a total of $(3M_r^2 + 2M_r)L$ multiplications in each round of training.

On the source side, according to (58), each source node takes M_s multiplications to compute beamforming signal $\mathbf{u}^{(m)} s^{(m)}$

TABLE I
THE NUMBER OF MULTIPLICATIONS CONDUCTED BY THE DISTRIBUTED NODES PER ROUND OF TRAINING

	forward propagation	back-propagation	Total
Source	$M_s L$	$3M_s L$	$4M_s L$
Relay	$M_r^2 L$	$(2M_r^2 + 2M_r)L$	$(3M_r^2 + 2M_r)L$
Destination	$M_d L$	$2M_d L$	$3M_d L$

in the forward propagation. In the backpropagation [cf. (65)], similar to the relay node, the source first needs $2M_s$ multiplications to compute $\frac{\partial \mathbf{x}^{(m)*}}{\partial \mathbf{z}^{(m)*}} \boldsymbol{\xi}_d^{(m)}$ and $\frac{\partial \mathbf{x}^{(m)}}{\partial \mathbf{z}^{(m)*}} \boldsymbol{\xi}_d^{(m)*}$, where $\boldsymbol{\xi}_d^{(m)} \triangleq \sum_{n=1}^N \mathbf{H}_r^{(n,m)H} (\mathbf{V}^{(n)} \frac{\partial J}{\partial \mathbf{b}^{(n)*}})$ is the received feedback signal. Then the source needs M_s multiplications to multiply $(\frac{\partial \mathbf{x}^{(m)*}}{\partial \mathbf{z}^{(m)*}} \boldsymbol{\xi}_d^{(m)} + \frac{\partial \mathbf{x}^{(m)}}{\partial \mathbf{z}^{(m)*}} \boldsymbol{\xi}_d^{(m)*})$ with $s^{(m)*}$ to obtain $\frac{\partial J}{\partial \mathbf{u}^{(m)*}}$. Therefore, the source performs a total of $4M_s L$ multiplications in each round of training.

We summarize in Table I the number of multiplications required by each node in each round of training, and we can see that the complexity of the DLRB scheme is quite moderate.

V. NUMERICAL SIMULATIONS

In this section, we verify the effectiveness of the proposed algorithms via numerical simulations. In the examples except for the last one, the source-to-relay channel and the relay-to-destination channel are assumed to be frequency-flat Rayleigh fading and remain static. The pilot sequence length $L = 32$. The nonlinear PA is simulated as the SEL function σ in (9).

Note that minimizing the MSE amounts to maximizing the output signal-to-noise ratio (SNR), because [36, Equation (13)]

$$SNR = \frac{1}{MSE} - 1. \tag{66}$$

Hence in the simulations we also use the output SNR/SINR of the destination as the metric to evaluate the performance of the system based on the average of 100 Monte Carlo trials. $\rho_{\text{dest}} (= \frac{NM_r}{\sigma_d^2})$ is the SNR of the relay-to-destination channel and $\rho_{\text{relay}} (= \frac{MM_s}{\sigma_r^2})$ is the SNR of the source-to-relay channel. The hyper-parameter and learning rate used in (37) – (42) are $\lambda = 0.9$ and $\alpha = 0.3$, respectively. Other parameters are given on the top of the figures.

In the first example, we simulate the DLRB algorithm to see the convergence of its MSE and SNR [cf. (66)] under different number of the relay nodes (N), and under different number of the antennas per relay node (M_r). Fig. 10 shows that most gain is achieved in the first 200 iterations, where one iteration represents one round of forward and backward training sessions as illustrated in Fig. 6. As expected, the output SNR/MSE improves as the number of relays and relay antennas increases. The network with one M_r -antenna relay outperforms the one with M_r single-antenna relays, which is not surprising since the relay processing matrix \mathbf{V} is constrained to be diagonal in the latter case.

For the subsequent simulations, the DLRB algorithm is based on 200 iterations. The centralized implementation as explained in Section III-C, however, uses 1000 iterations since it runs in a

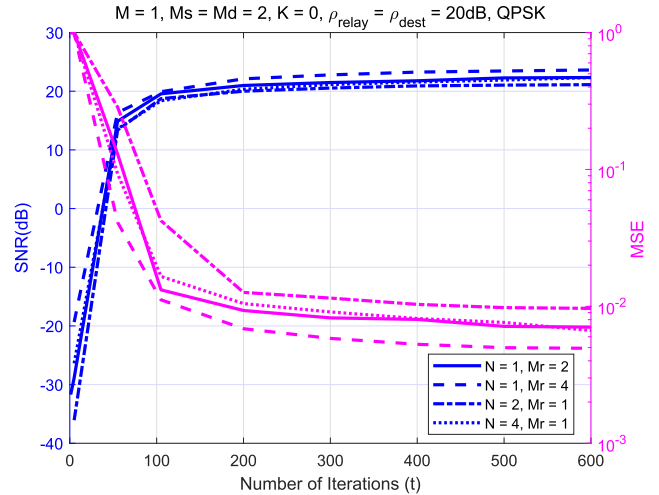


Fig. 10. Output SNR of the relay network achieved by the DLRB scheme as the number of iterations with respect to different number of the relay nodes and the relay antennas.

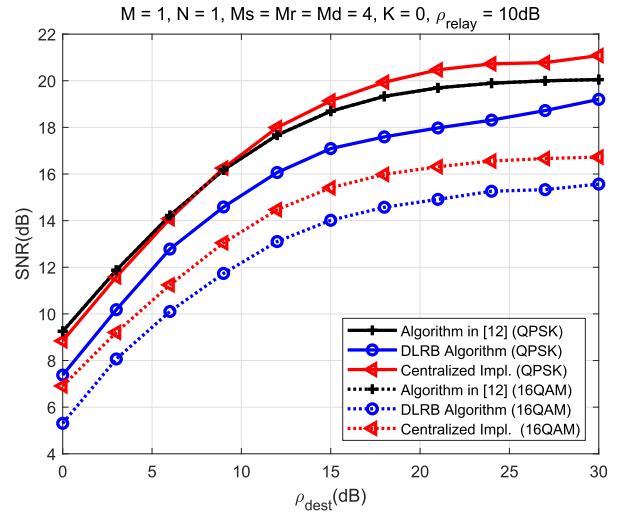


Fig. 11. Comparison between the proposed algorithms with the algorithm in [12] in the output SNR of the destination.

CPU and consumes no communication resources. To differentiate the two proposed algorithms, we use ‘Centralized Impl.’ and ‘DLRB algorithm’ to denote the centralized and the distributed implementations, respectively.

In the second simulation, we include the ‘‘Optimal Unquantized Scheme’’ proposed in [12], which is designed to optimize the linear AF relay network with a single relay node with the average power constraint but is not subject to the PA saturation. In contrast, our proposed algorithms impose the instantaneous power constraint [cf. (6)], which is more stringent (and more realistic). Under this unfair comparison, it is not surprising to see from Fig. 11 that the optimal unquantized scheme of [12] (labeled as ‘Algorithm in [12]’) can outperform our proposed algorithms, especially for 16QAM, a non-constant modulus signal. Fig. 11 shows that for the QPSK signal the proposed algorithms can even outperform the linear AF scheme in the low SNR regime, because clipping the QPSK signal at the relay

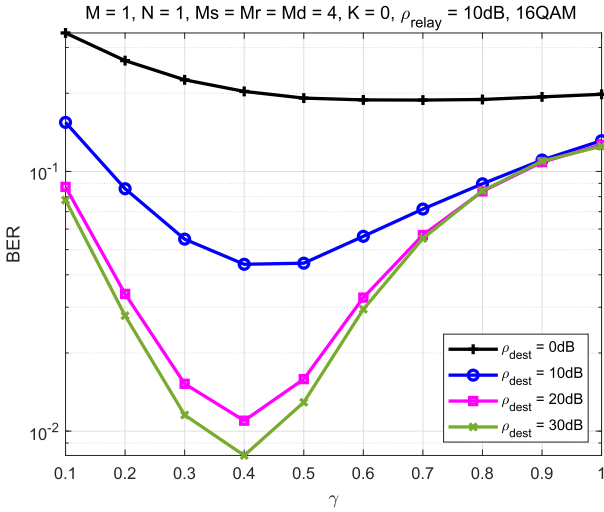


Fig. 12. BER of the algorithm in [12] versus the power constraints value after the PA.

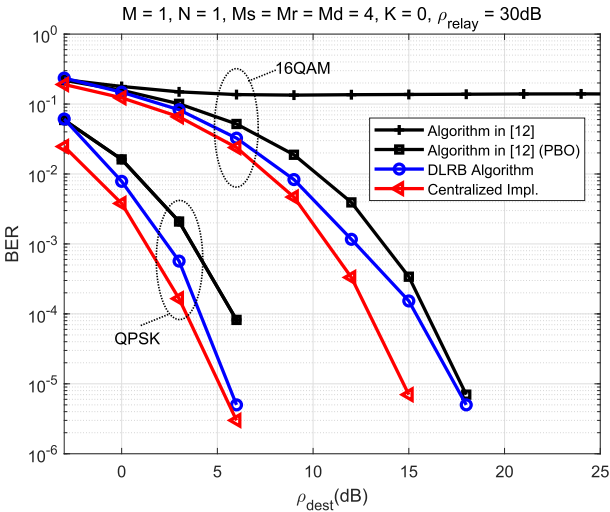


Fig. 13. BER of the proposed algorithms and the algorithm in [12] with and without the optimized power constraints in the presence of the PA.

nodes helps reduce the noise. The performance of the DLRB algorithm is inferior to the centralized implementation because it conducted fewer forward-and-backward iterations.

In the presence of nonlinear PAs, the optimal unquantized scheme of [12] needs to be modified to avoid PA saturation. More specifically, the transmitted non-constant modulus signal should be power backoff-ed. Fig. 12 shows the BER results of the 16QAM signal transmitted using the scheme in [12] under different power backoff coefficients $\gamma \in (0, 1)$. One can choose the optimal power backoff (PBO) for the scheme in [12] to minimize the BER.

In Fig. 13, we compare our proposed algorithms with the linear AF with optimal power backoff (labeled as ‘Algorithm in [12] (PBO)’ and the original scheme in [12], all subject to the nonlinear PA. In this fair comparison, our proposed algorithms consistently outperform the linear AF scheme.

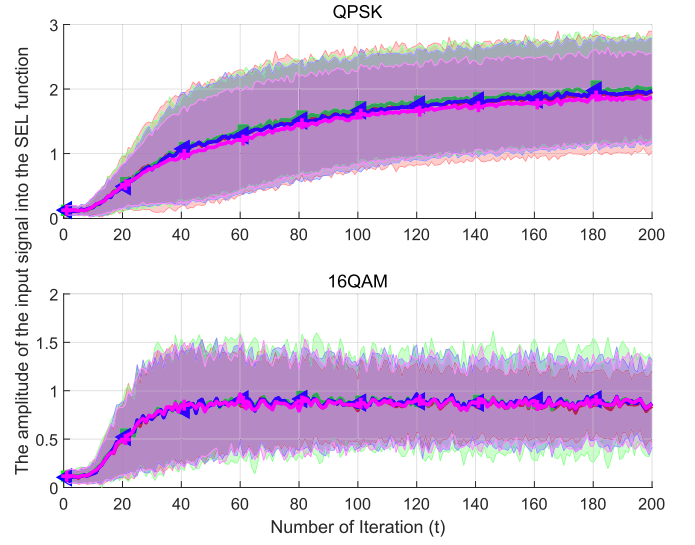


Fig. 14. The amplitude of the input signal into the SEL function as the number of iterations for QPSK and 16QAM signals.

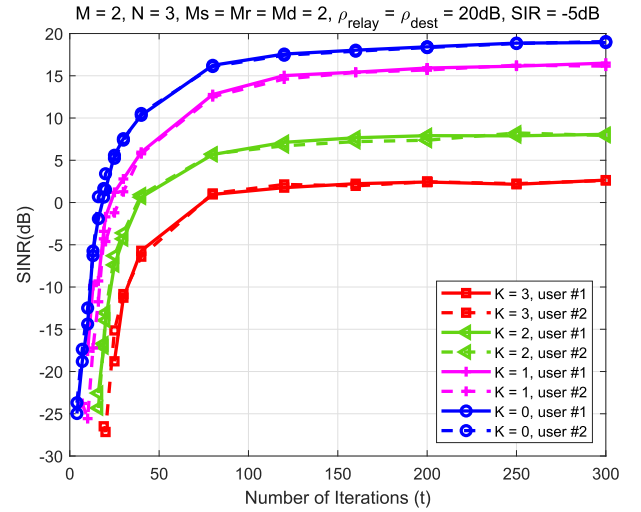


Fig. 15. Output SINR of the destination with respect to different number of the interferences.

Then we run a simulation with setting $M = N = 1$, $M_s = M_r = M_d = 4$, $K = 0$, and $\rho_1 = \rho_2 = 10\text{dB}$. Fig. 14 shows a continuous error bar diagram of the amplitude $|\mathbf{b}|$ [cf. (8)], where \mathbf{b} is the input into the SEL function. The solid line in the middle represents the mean, and the shaded parts represent $|\mathbf{b}|$ within its one standard deviation. We can see that $|\mathbf{b}| > 1$ with high probability, which shows that the relay node actually aggressively enters the nonlinear regime of the SEL function.

We then simulate the DLRB algorithm under interferences. Fig. 15 shows that a network with 2 two-antenna users and 3 two-antenna relays running the DLRB algorithm can suppress up to 3 interferences owing to the inter-relay coordination. In other words, the relay nodes can coordinate to form a virtual array for interference suppression, but without information exchange between the relay nodes.

In the previous simulations, we have assumed that the back-propagation from the destinations to the relay nodes and from

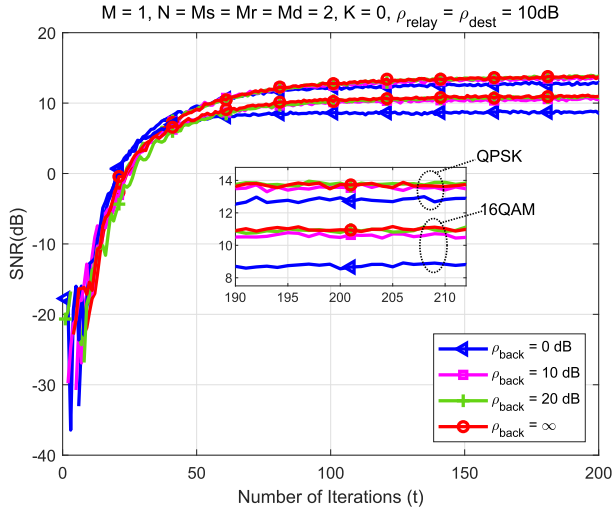


Fig. 16. Output SNR of the destination as the number of iterations with and without noise in the reverse channel.

the relays to the sources are noise-free in the DLRB algorithm. Now we consider a more realistic scenario where in the reverse channel the destinations’ and the relays’ broadcasting of the sequences $[\mathbf{w}^{(m)}(\hat{s}^{(m)} - s^{(m)})]^*$, $m = 1, \dots, M$ and $[\mathbf{V}^{(n)} \frac{\partial J}{\partial \mathbf{b}^{(n)*}}]^*$, $n = 1, \dots, N$ are contaminated by the noise $\zeta_d \sim \mathcal{CN}(0, \sigma_{\zeta_d}^2 \mathbf{I})$ and $\zeta_r \sim \mathcal{CN}(0, \sigma_{\zeta_r}^2 \mathbf{I})$, respectively. The SNRs of the reverse channel is defined as

$$\rho_{\text{back}1} \triangleq \frac{MM_d}{\sigma_{\zeta_d}^2}, \text{ and } \rho_{\text{back}2} \triangleq \frac{NM_r}{\sigma_{\zeta_r}^2}. \quad (67)$$

Fig. 16 shows that even when $\rho_{\text{back}1} = \rho_{\text{back}2} = 0\text{dB}$, the output SNRs for QPSK and 16QAM signals are only about 1 dB and 2 dB lower than those without noise, respectively. It verifies that the DLRB algorithm is robust to the noise in the back-propagation channel, owing to the average operations in (34)–(36).

In the last example, we consider the more practical scenario where the channels are time-varying. Specifically, we set that the carrier frequency $f_c = 2.4\text{GHz}$, the bandwidth $B = 20\text{MHz}$, i.e., the Nyquist sampling duration $T_s = \frac{1}{B} = \frac{1}{20 \times 10^6} = 50\text{ns}$, and the channel mobility speed $v = 40\text{km/h}$, i.e., the Doppler frequency spread $f_d = \frac{v}{c} f_c = \frac{40/3.6}{2 \times 10^8} \times 2.4 \times 10^9 \approx 88\text{Hz}$. According to the frame structure in Fig. 6, the DLRB scheme needs a total of $2(T + 1)LT_s$ seconds for training. And in the initialization stage the DLRB scheme needs 64 iterations for training that last for 0.208 ms, i.e., $2 \times (64 + 1) \times 32 \times 50 \times 10^{-9} = 0.208\text{ms}$, before transmitting 128 sets of data; based on the first phase, the subsequent training phases are warm-started, and hence require much fewer rounds of training as shown in Fig. 7. Indeed, the subsequent training only needs 4 iterations that take only 0.016 ms, i.e., $2 \times (4 + 1) \times 32 \times 50 \times 10^{-9} = 0.016\text{ms}$, followed by 128 sets of data payload. As shown in Fig. 17, the red curve is the pilot training phase and the blue is the data transmission phase. The four curves, from the upper to the lower, correspond to the case of $K = 0$ (no) interference to $K = 3$ interferences. After the first training session, although the

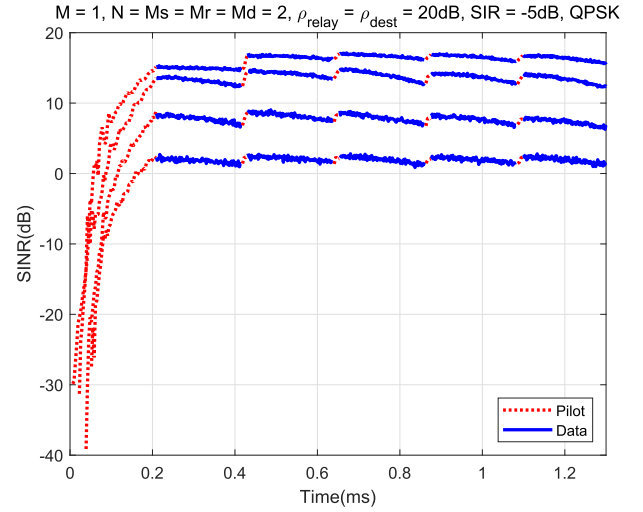


Fig. 17. Output SINR of the destination for the time-vary channels as the time with respect to different number of the interferences.

performance of data transmission will slowly degenerate owing to the time varying channel, it only needs 4 iterations of training to compensate for the SINR loss occurred in the preceding data transmission. Overall, the network takes only a moderate portion of time resource for the network training. We can also see that the DLRB algorithm can not only adapt to the changes of the channels, but also suppress the interferences from the unknown time-varying channels.

VI. CONCLUSION

This paper presents a novel perspective of regarding a relay network as a four-layer “quasi-neural network” and proposes a Distributed Learning based Relay Beamforming (DLRB) algorithm for the relay network. We adopt a soft envelop limiter (SEL) for instantaneous power constrain per antenna to avoid the distortion of the nonlinear power amplifier (PA). The proposed DLRB scheme can optimize the weights of the distributed nodes assuming no channel state information (CSI). The optimization is conducted via having the sources transmit pilot sequences, and having the destinations and the relays broadcast some beamformed derivatives through the reverse channel – the relay/source/destination nodes exchange no data between their peers. We also present a frame design to support the DRLB so that it can adapt well with time-varying channels. The extensive simulations verify the effectiveness of the proposed algorithms in both with interference and interference-free environments. And the proposed algorithms can outperform the state-of-the-art method that ignores the nonlinearity of the PAs.

We believe that this work opens up several interesting avenues for future exploration. One would be to extend to the more realistic case of orthogonal frequency division multiplexing (OFDM) scenario to accommodate for frequency selective channels; and another possible way is to extend the single-stream case studied in this paper to multi-stream cases.

APPENDIX
PROOF TO PROPOSITION III.1

We first reproduce the following definition and lemma from [37].

Definition VI.1: [37, Definition 2.2] Let $z = x + jy$, where $x, y \in \mathbb{R}$, then the formal derivatives with respect to z and z^* of $f(z_0)$ at $z_0 \in \mathbb{C}$ are defined as

$$\frac{\partial f(z_0)}{\partial z} = \frac{1}{2} \left(\frac{\partial f(z_0)}{\partial x} - j \frac{\partial f(z_0)}{\partial y} \right), \quad (68)$$

and

$$\frac{\partial f(z_0)}{\partial z^*} = \frac{1}{2} \left(\frac{\partial f(z_0)}{\partial x} + j \frac{\partial f(z_0)}{\partial y} \right). \quad (69)$$

In calculating $\frac{\partial f(z_0)}{\partial z}$ and $\frac{\partial f(z_0)}{\partial z^*}$, the variables z and z^* are treated as independent variables.

Lemma VI.2: [37, Theorem 3.3] Let $f : \mathbb{C}^{N \times Q} \times \mathbb{C}^{N \times Q} \rightarrow \mathbb{R}$. Then the following holds:

$$\mathcal{D}_{\mathbf{Z}^*} f = (\mathcal{D}_{\mathbf{Z}} f)^*. \quad (70)$$

Now we establish the following lemma.

Lemma VI.3: Derivatives of SEL function, $a = \sigma(b) = \begin{cases} b & |b| \leq 1 \\ e^{j\angle b} & |b| > 1 \end{cases} \in \mathbb{C}$, are

$$\frac{\partial a}{\partial b^*} = \begin{cases} 0 & |b| \leq 1 \\ -\frac{1}{2|b|} e^{j2\angle b} & |b| > 1 \end{cases}, \quad (71)$$

and

$$\frac{\partial a^*}{\partial b^*} = \begin{cases} 1 & |b| \leq 1 \\ \frac{1}{2|b|} & |b| > 1 \end{cases}. \quad (72)$$

where $\angle b$ represents the angle of b .

Proof: When $|b| \leq 1$,

$$\frac{\partial a}{\partial b^*} = \frac{\partial b}{\partial b^*} = 0, \quad \text{and} \quad \frac{\partial a^*}{\partial b^*} = \frac{\partial b^*}{\partial b^*} = 1; \quad (73)$$

when $|b| > 1$,

$$\begin{aligned} \frac{\partial a}{\partial b^*} &= \frac{\partial e^{j\angle b}}{\partial b^*} = \frac{\partial \frac{b}{|b|}}{\partial b^*} \\ &= \left(\frac{\partial b}{\partial b^*} \right) |b|^{-1} + b \left(\frac{\partial |b|^{-1}}{\partial b^*} \right) \\ &= 0 - b |b|^{-2} \frac{\partial |b|}{\partial b^*} \\ &= -\frac{1}{2|b|} e^{j2\angle b}, \end{aligned} \quad (74)$$

and

$$\begin{aligned} \frac{\partial a^*}{\partial b^*} &= \frac{\partial e^{-j\angle b}}{\partial b^*} = \frac{\partial \frac{b^*}{|b|}}{\partial b^*} \\ &= \left(\frac{\partial b^*}{\partial b^*} \right) |b|^{-1} + b^* \left(\frac{\partial |b|^{-1}}{\partial b^*} \right) \end{aligned}$$

$$\begin{aligned} &= |b|^{-1} - b^* |b|^{-2} \left(\frac{\partial |b|}{\partial b^*} \right) \\ &= \frac{1}{2|b|}, \end{aligned} \quad (75)$$

where

$$\frac{\partial |b|}{\partial b^*} = \frac{\partial (b^* b)^{\frac{1}{2}}}{\partial b^*} = \frac{1}{2} (b^* b)^{-\frac{1}{2}} \frac{\partial b^* b}{\partial b^*} = \frac{b}{2|b|} = \frac{e^{j\angle b}}{2}. \quad (76)$$

Now we are ready to prove Proposition III.1.

According to the chain rule of derivative and Lemma VI.2,

$$\frac{\partial J}{\partial \mathbf{w}^*} = \frac{\partial \hat{s}}{\partial \mathbf{w}^*} \frac{\partial J}{\partial \hat{s}} = \frac{\partial \hat{s}}{\partial \mathbf{w}^*} \left(\frac{\partial J}{\partial \hat{s}^*} \right)^*. \quad (77)$$

Since it follows from (13) that $\frac{\partial \hat{s}}{\partial \mathbf{w}^*} = \mathbf{y}$, (77) can be reformulated as (16). And (17) follows immediately from (15).

According to the chain rule of derivative [cf. (8)],

$$\begin{aligned} \frac{\partial J}{\partial \mathbf{V}^*} &= \left(\frac{\partial J}{\partial \mathbf{v}_1^*}, \frac{\partial J}{\partial \mathbf{v}_2^*}, \dots, \frac{\partial J}{\partial \mathbf{v}_{M_r}^*} \right) \\ &= \left(\frac{\partial b_1}{\partial \mathbf{v}_1^*} \frac{\partial J}{\partial b_1}, \frac{\partial b_2}{\partial \mathbf{v}_2^*} \frac{\partial J}{\partial b_2}, \dots, \frac{\partial b_{M_r}}{\partial \mathbf{v}_{M_r}^*} \frac{\partial J}{\partial b_{M_r}} \right), \end{aligned} \quad (78)$$

where $\frac{\partial b_q}{\partial \mathbf{v}_q^*} = \mathbf{r}$, $q = 1, \dots, M_r$; thus, (78) is deduced to

$$\frac{\partial J}{\partial \mathbf{V}^*} = \left(\mathbf{r} \frac{\partial J}{\partial b_1}, \mathbf{r} \frac{\partial J}{\partial b_2}, \dots, \mathbf{r} \frac{\partial J}{\partial b_{M_r}} \right) = \mathbf{r} \left(\frac{\partial J}{\partial \mathbf{b}^*} \right)^H, \quad (79)$$

which has proven (18).

As for $\frac{\partial J}{\partial \mathbf{b}^*}$ in (18), according to the chain rule,

$$\frac{\partial J}{\partial \mathbf{b}^*} = \frac{\partial \mathbf{a}^*}{\partial \mathbf{b}^*} \frac{\partial J}{\partial \mathbf{a}^*} + \frac{\partial \mathbf{a}}{\partial \mathbf{b}^*} \frac{\partial J}{\partial \mathbf{a}} \in \mathbb{C}^{M_r}, \quad (80)$$

i.e., (19), where

$$\frac{\partial J}{\partial \mathbf{a}^*} = \frac{\partial \hat{s}^*}{\partial \mathbf{a}^*} \frac{\partial J}{\partial \hat{s}^*}. \quad (81)$$

Combining (4) and (13) leads to

$$\hat{s} = \mathbf{w}^H \mathbf{H}_d \mathbf{a} + \mathbf{w}^H \boldsymbol{\eta}_d, \quad (82)$$

from which we obtain

$$\frac{\partial \hat{s}^*}{\partial \mathbf{a}^*} = \mathbf{H}_d^H \mathbf{w}. \quad (83)$$

Inserting (83) into (81) yields (20).

Since $\mathbf{a} = \sigma(\mathbf{b})$ [cf. (12)] is an element-wise function of \mathbf{b} , i.e., $a_q = \sigma(b_q)$, $q = 1, \dots, M_r$, $\frac{\partial \mathbf{a}^*}{\partial \mathbf{b}^*}$ and $\frac{\partial \mathbf{a}}{\partial \mathbf{b}^*}$ are diagonal as shown in (21) and (22), where $\frac{\partial a_q}{\partial b_q^*}$ and $\frac{\partial a_q}{\partial b_q}$ in (23) and (24) can be obtained from Lemma VI.3.

Inserting (20)–(22) into (19) leads to $\frac{\partial J}{\partial \mathbf{b}^*}$, so we can obtain $\frac{\partial J}{\partial \mathbf{V}^*}$ as shown in (18).

According to the chain rule of derivative, we can prove (25) as

$$\frac{\partial J}{\partial \mathbf{u}^*} = \frac{\partial \mathbf{z}^H}{\partial \mathbf{u}^*} \frac{\partial J}{\partial \mathbf{z}^*} \stackrel{(a)}{=} \mathbf{s}^* \frac{\partial J}{\partial \mathbf{z}^*}, \quad (84)$$

where $\stackrel{(a)}{=}$ holds because $\frac{\partial \mathbf{z}^H}{\partial \mathbf{u}^*} = \mathbf{s}^* \mathbf{I}_{M_s}$ [cf. (7)].

As for $\frac{\partial J}{\partial \mathbf{z}^*}$ in (25), we can use the chain rule of derivative to obtain (26) as

$$\frac{\partial J}{\partial \mathbf{z}^*} = \frac{\partial \mathbf{x}^*}{\partial \mathbf{z}^*} \frac{\partial J}{\partial \mathbf{x}^*} + \frac{\partial \mathbf{x}}{\partial \mathbf{z}^*} \frac{\partial J}{\partial \mathbf{x}}, \quad (85)$$

and (27) as

$$\frac{\partial J}{\partial \mathbf{x}^*} = \frac{\partial \mathbf{b}^H}{\partial \mathbf{x}^*} \frac{\partial J}{\partial \mathbf{b}^*} \stackrel{(b)}{=} \mathbf{H}_r^H \mathbf{V} \frac{\partial J}{\partial \mathbf{b}^*}, \quad (86)$$

where $\stackrel{(b)}{=}$ holds because $\frac{\partial \mathbf{b}^H}{\partial \mathbf{x}^*} = \mathbf{H}_r^H \mathbf{V}$, as combining (2) and (8) leads to $\mathbf{b} = \mathbf{V}^H \mathbf{H}_r \mathbf{x} + \mathbf{V}^H \boldsymbol{\eta}_r$.

Since $\mathbf{x} = \sigma(\mathbf{z})$ just like $\mathbf{a} = \sigma(\mathbf{b})$, following the same proof of (21), (22), (23), and (24), we can prove (28), (29), (30), and (31).

Inserting (27)–(29) into (26) leads to $\frac{\partial J}{\partial \mathbf{z}^*}$; thus, we can obtain $\frac{\partial J}{\partial \mathbf{u}^*}$ as shown in (25).

REFERENCES

- [1] B. Wang, J. Zhang, and A. Host-Madsen, "On the capacity of MIMO relay channels," *IEEE Trans. Inf. Theory*, vol. 51, no. 1, pp. 29–43, Jan. 2005.
- [2] E. Che, H. D. Tuan, and H. H. Nguyen, "Joint optimization of cooperative beamforming and relay assignment in multi-user wireless relay networks," *IEEE Trans. Wireless Commun.*, vol. 13, no. 10, pp. 5481–5495, Oct. 2014.
- [3] Y. Zeng, R. Zhang, and T. J. Lim, "Throughput maximization for UAV-enabled mobile relaying systems," *IEEE Trans. Commun.*, vol. 64, no. 12, pp. 4983–4996, Dec. 2016.
- [4] Z. Fang, Y. Lu, and W. Zheng, "Design and implement of a relayed assisted emergency wireless communication system," in *Proc. IEEE Int. Conf. Comput. Commun. Eng. Technol.*, 2018, pp. 68–72.
- [5] S. A. Ayoughi and W. Yu, "Interference mitigation via relaying," *IEEE Trans. Inf. Theory*, vol. 65, no. 2, pp. 1137–1152, Feb. 2019.
- [6] I. Guvenc, U. Kozat, M.-R. Jeong, F. Watanabe, and C.-C. Chong, "Reliable multicast and broadcast services in relay-based emergency communications," *IEEE Wireless Commun.*, vol. 15, no. 3, pp. 40–47, Mar. 2008.
- [7] D.-H. Tran, V.-D. Nguyen, S. Gautam, S. Chatzinotas, T. X. Vu, and B. Ottersten, "UAV relay-assisted emergency communications in IoT networks: Resource allocation and trajectory optimization," *IEEE Trans. Wireless Commun.*, early access, 2020, doi: [10.1109/TWC.2021.3105821](https://doi.org/10.1109/TWC.2021.3105821).
- [8] H. Baek and J. Lim, "Design of future UAV-relay tactical data link for reliable UAV control and situational awareness," *IEEE Commun. Mag.*, vol. 56, no. 10, pp. 144–150, Oct. 2018.
- [9] J.-K. Lee, K.-M. Lee, H.-J. Noh, and J. Lim, "A cooperative relay scheme for tactical multi-hop wireless networks," in *Proc. IEEE Mil. Commun. Conf.*, 2013, pp. 527–532.
- [10] J.-H. Lee, "Optimal power allocation for physical layer security in multi-hop DF relay networks," *IEEE Trans. Wireless Commun.*, vol. 15, no. 1, pp. 28–38, Jan. 2016.
- [11] G. Zheng, K.-K. Wong, A. Paulraj, and B. Ottersten, "Collaborative-relay beamforming with perfect CSI: Optimum and distributed implementation," *IEEE Signal Process. Lett.*, vol. 16, no. 4, pp. 257–260, Apr. 2009.
- [12] B. Khoshnevis, W. Yu, and R. Adve, "Grassmannian beamforming for MIMO amplify-and-forward relaying," *IEEE J. Sel. Areas Commun.*, vol. 26, no. 8, pp. 1397–1407, Aug. 2008.
- [13] Y. Jing and H. Jafarkhani, "Network beamforming using relays with perfect channel information," *IEEE Trans. Inf. Theory*, vol. 55, no. 6, pp. 2499–2517, Jun. 2009.
- [14] M. Zhang, H. Yi, H. Yu, H. Luo, and W. Chen, "Joint optimization in bidirectional multi-user multi-relay MIMO systems: Non-robust and robust cases," *IEEE Trans. Veh. Technol.*, vol. 62, no. 7, pp. 3228–3244, Sep. 2013.
- [15] G. Zheng, K.-K. Wong, A. Paulraj, and B. Ottersten, "Robust collaborative-relay beamforming," *IEEE Trans. Signal Process.*, vol. 57, no. 8, pp. 3130–3143, Aug. 2009.
- [16] V. Havary-Nassab, S. Shahbazpanahi, A. Grami, and Z.-Q. Luo, "Distributed beamforming for relay networks based on second-order statistics of the channel state information," *IEEE Trans. Signal Process.*, vol. 56, no. 9, pp. 4306–4316, Sep. 2008.
- [17] J. Li, A. P. Petropulu, and H. V. Poor, "Cooperative transmission for relay networks based on second-order statistics of channel state information," *IEEE Trans. Signal Process.*, vol. 59, no. 3, pp. 1280–1291, Mar. 2011.
- [18] M. A. M. Sadr, M. A. Attari, and R. Amiri, "Robust relay beamforming against jamming attack," *IEEE Commun. Lett.*, vol. 22, no. 2, pp. 312–315, Feb. 2018.
- [19] G. Kramer, M. Gastpar, and P. Gupta, "Cooperative strategies and capacity theorems for relay networks," *IEEE Trans. Inf. Theory*, vol. 51, no. 9, pp. 3037–3063, Sep. 2005.
- [20] J. N. Laneman and G. W. Wornell, "Cooperative diversity in wireless networks: Algorithms and architectures," Ph.D. dissertation, Massachusetts Inst. Technol., 2002.
- [21] K. Eltira, N. Jibreel, A. Younis, and R. Mesleh, "Capacity analysis of cooperative amplify and forward multiple-input multiple-output systems," *Trans. Emerg. Telecommun. Technol.*, vol. 31, no. 10, Oct. 2021, Art. no. e4290.
- [22] Y. Shim, W. Choi, and H. Park, "Beamforming design for full-duplex two-way amplify-and-forward MIMO relay," *IEEE Trans. Wireless Commun.*, vol. 15, no. 10, pp. 6705–6715, Oct. 2016.
- [23] D. Simmons, D. Halls, and J. P. Coon, "OFDM-based nonlinear fixed-gain amplify-and-forward relay systems: SER optimization and experimental testing," in *Proc. Eur. Conf. Netw. Commun.*, 2014, pp. 1–5.
- [24] D. E. Simmons and J. P. Coon, "Two-way OFDM-based nonlinear amplify-and-forward relay systems," *IEEE Trans. Veh. Technol.*, vol. 65, no. 5, pp. 3808–3812, May 2016.
- [25] M. Majidi, A. Mohammadi, A. Abdipour, and M. Valkama, "Characterization and performance improvement of cooperative wireless networks with nonlinear power amplifier at relay," *IEEE Trans. Veh. Technol.*, vol. 69, no. 3, pp. 3244–3255, Mar. 2020.
- [26] R. Wang and Y. Jiang, "An interference-resilient relay beamforming scheme inspired by back-propagation algorithm," in *Proc. Inf. Theory Appl. Workshop*, 2020, pp. 1–6.
- [27] R. Wang and Y. Jiang, "A nonlinear relay scheme resilient to interference with unknown CSI," in *Proc. 54th Asilomar Conf. Signals, Syst., Comput.*, 2020, pp. 485–489.
- [28] J. Guerreiro, R. Dinis, and P. Montezuma, "Analytical evaluation of nonlinear amplify-and-forward relay systems for OFDM signals," in *Proc. IEEE 80th Veh. Technol. Conf.*, 2014, pp. 1–5.
- [29] T. Riihonen, S. Werner, F. Gregorio, R. Wichman, and J. Hamalainen, "BEP analysis of OFDM relay links with nonlinear power amplifiers," in *Proc. IEEE Wireless Commun. Netw. Conf.*, 2010, pp. 1–6.
- [30] I. Goodfellow, Y. Bengio, and A. Courville, *Deep Learning*. Cambridge, MA, USA: MIT Press, 2016. [Online]. Available: <http://www.deeplearningbook.org>
- [31] D. Dardari, V. Tralli, and A. Vaccari, "A theoretical characterization of nonlinear distortion effects in OFDM systems," *IEEE Trans. Commun.*, vol. 48, no. 10, pp. 1755–1764, Oct. 2000.
- [32] M. G. El-Mashed, "Effect of HPAs and phase noise problems on the multi-pair massive antenna relaying systems," *Digit. Signal Process.*, vol. 84, pp. 46–58, 2019.
- [33] E. Perahia and R. Stacey, *Next Generation Wireless LANs: 802.11n and 802.11ac*, 2nd ed. Cambridge, U.K.: Cambridge Univ. Press, 2013.
- [34] L. Schenato and F. Fiorentin, "Average timesynch: A consensus-based protocol for clock synchronization in wireless sensor networks," *Automatica*, vol. 47, no. 9, pp. 1878–1886, 2011.
- [35] R. Yang and Y. Jiang, "Consensus-based clock synchronization for wide area networks," in *Proc. IEEE Wireless Commun. Netw. Conf.*, 2021, pp. 1–6.
- [36] D. Guo, S. Shamai, and S. Verdú, "Mutual information and minimum mean-square error in Gaussian channels," *IEEE Trans. Inf. Theory*, vol. 51, no. 4, pp. 1261–1282, Apr. 2005.
- [37] A. Hjørungnes, *Complex-Valued Matrix Derivatives: With Applications in Signal Processing and Communications*. Cambridge, U.K.: Cambridge Univ. Press, 2011.



Rui Wang (Graduate Student Member, IEEE) received the B.S. degree in communication engineering from Northeastern University, Shenyang, China, in 2018. She is currently working toward the Ph.D. degree with the Department of Communication Science and Engineering, Fudan University, Shanghai, China. Her research interests include MIMO wireless communication, relay network, and signal processing for wireless communication.



Yi Jiang (Member, IEEE) received the B.S. degree in electrical engineering and information science from the University of Science and Technology of China, Hefei, China, in 2001, and the M.S. and Ph.D. degrees in electrical engineering from the University of Florida, Gainesville, FL, USA, in 2003 and 2005, respectively. In 2005, he was a Research Consultant with Information Science Technologies Inc., Fort Collins, CO, USA. From 2005 to 2007, he was a Post-doctoral Researcher with the University of Colorado, Boulder CO. He moved to San Diego, CA, USA, in

2007, and was with multiple companies, including NextWave Wireless from May 2007 to July 2008, Qualcomm Corporate Research and Development from August 2008 to May 2012, IAA Incorporated from June 2012 to January 2013, and Silvus Technologies from February 2013 to July 2016. He also was an Adjunct Researcher with the Electrical Engineering Department, University of California, Los Angeles, CA, from October 2014 to July 2016. He joined Fudan University, Shanghai, China, in August 2016, and he is currently a Professor with the Department of Communication Science and Engineering, Fudan University. His research interests include array signal processing and mobile ad hoc networks. He is the Editor of IEEE WIRELESS COMMUNICATIONS LETTERS.



Wei Zhang (Fellow, IEEE) received the Ph.D. degree from The Chinese University of Hong Kong, Hong Kong, in 2005. He is currently a Professor with the School of Electrical Engineering and Telecommunications, University of New South Wales, Sydney, NSW, Australia. His current research interests include UAV communications, 5G and beyond. He received six best paper awards from IEEE conferences and ComSoc technical committees. He was elevated to Fellow of the IEEE in 2015, and was an IEEE ComSoc Distinguished Lecturer in 2016–2017.

Within the IEEE ComSoc, he has taken many leadership positions including Member-at-Large on the Board of Governors (2018–2020), the Chair of Wireless Communications Technical Committee (2019–2020), the Vice Director of Asia Pacific Board (2016–2021), the Editor-in-Chief of IEEE WIRELESS COMMUNICATIONS LETTERS (2016–2019), the Technical Program Committee Chair of APCC 2017 and ICC 2019, Award Committee Chair of Asia Pacific Board and Award Committee Chair of Technical Committee on Cognitive Networks. He was recently elected as the Vice President of IEEE Communications Society (2022–2023).

In addition, he was a Member in various ComSoc boards/standing committees, including Journals Board, Technical Committee Recertification Committee, Finance Standing Committee, Information Technology Committee, Steering Committee of IEEE TRANSACTIONS ON GREEN COMMUNICATIONS and Networking and Steering Committee of IEEE NETWORKING LETTERS. He is currently an Area Editor of IEEE TRANSACTIONS ON WIRELESS COMMUNICATIONS and the Editor-in-Chief of *Journal of Communications and Information Networks*. Previously, he was the Editor of IEEE TRANSACTIONS ON COMMUNICATIONS, IEEE TRANSACTIONS ON WIRELESS COMMUNICATIONS, IEEE TRANSACTIONS ON COGNITIVE COMMUNICATIONS AND NETWORKING, and IEEE JOURNAL ON SELECTED AREAS IN COMMUNICATIONS-COGNITIVE RADIO SERIES.